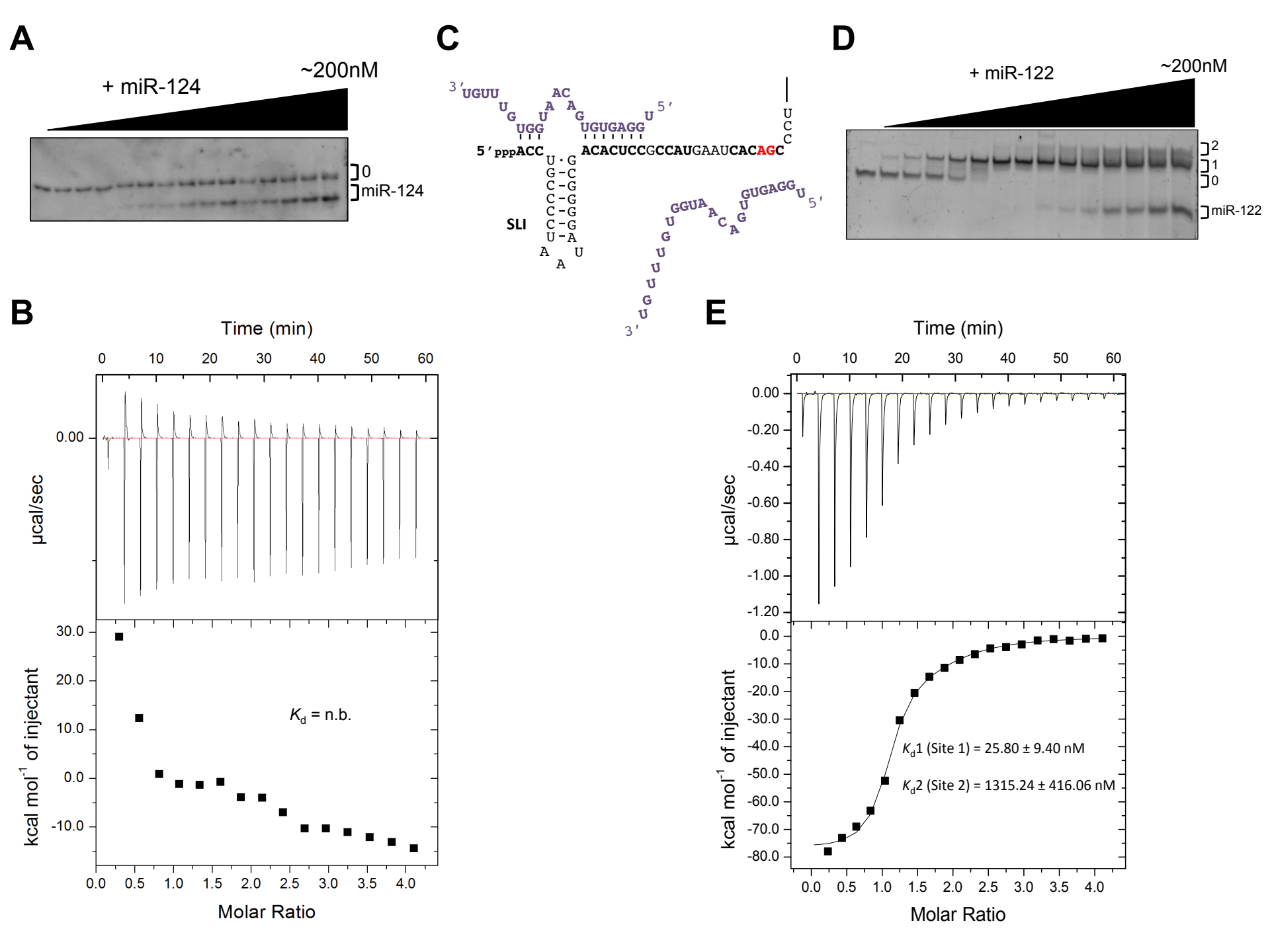
A
+ miR-124
~200nM
0
miR-124
C
3′UGUU
AC
U A A
G U G
U 5′
UGG
UGUGAGG
UCC
5′pppACC
ACACUCCGCCAUGAAUCACAGC
U·G
G-C
C-G
C-G
C-G
C-G
U-A
A U
A
SLI
GGUA
U
G
U
U
U
G
U
3′
GUGAGG
U 5′
D
+ miR-122
~200nM
2
1
0
miR-122
B
Time (min)
0 10 20 30 40 50 60
0.00
µcal/sec
30.0
20.0
10.0
0.0
-10.0
kcal mol-1 of injectant
Kd = n.b.
0.0 0.5 1.0 1.5 2.0 2.5 3.0 3.5 4.0
Molar Ratio
E
Time (min)
0 10 20 30 40 50 60
0.00
-0.20
-0.40
-0.60
-0.80
-1.00
-1.20
µcal/sec
0.0
-10.0
-20.0
-30.0
-40.0
-50.0
-60.0
-70.0
-80.0
kcal mol-1 of injectant
Kd1 (Site 1) = 25.80 ± 9.40 nM
Kd2 (Site 2) = 1315.24 ± 416.06 nM
0.0 0.5 1.0 1.5 2.0 2.5 3.0 3.5 4.0
Molar Ratio

Supplementary Figure S1. miR-124 does not interact with the HCV 5' terminus and miR-122 binds with higher affinity to Site 1 in 1-42 nt HCV RNA. (A) Non-denaturing gel electrophoresis mobility shit assay (EMSA) of 1-42 nt HCV RNA and increasing amounts of miR-124. **(B)** Thermogram and resulting binding curve of the titration of 1-42 nt HCV RNA with native miR-124. n.b. = no binding. **(C)** Model of the interaction of miR-122 (purple) and the 1-42 nt of the HCV Site 2p3,4 mutant (black), containing mutations in positions 3 and 4 of the miR-122 seed sequence of Site 2 (red). **(D)** Non-denaturing gel electrophoresis mobility shit assay (EMSA) of 1-42 nt HCV Site 2p3,4 RNA and increasing amounts of miR-122. **(E)** Thermogram and resulting binding curve of the titration of 1-42 nt HCV Site2p3,4 with miR-122. Affinities of each binding Site (K_d1, Site 1 and K_d2, Site 2) are indicated. All data are representative of at least three independent replicates and K_d values are an average of three measurements (±) error propagated from individual fits.

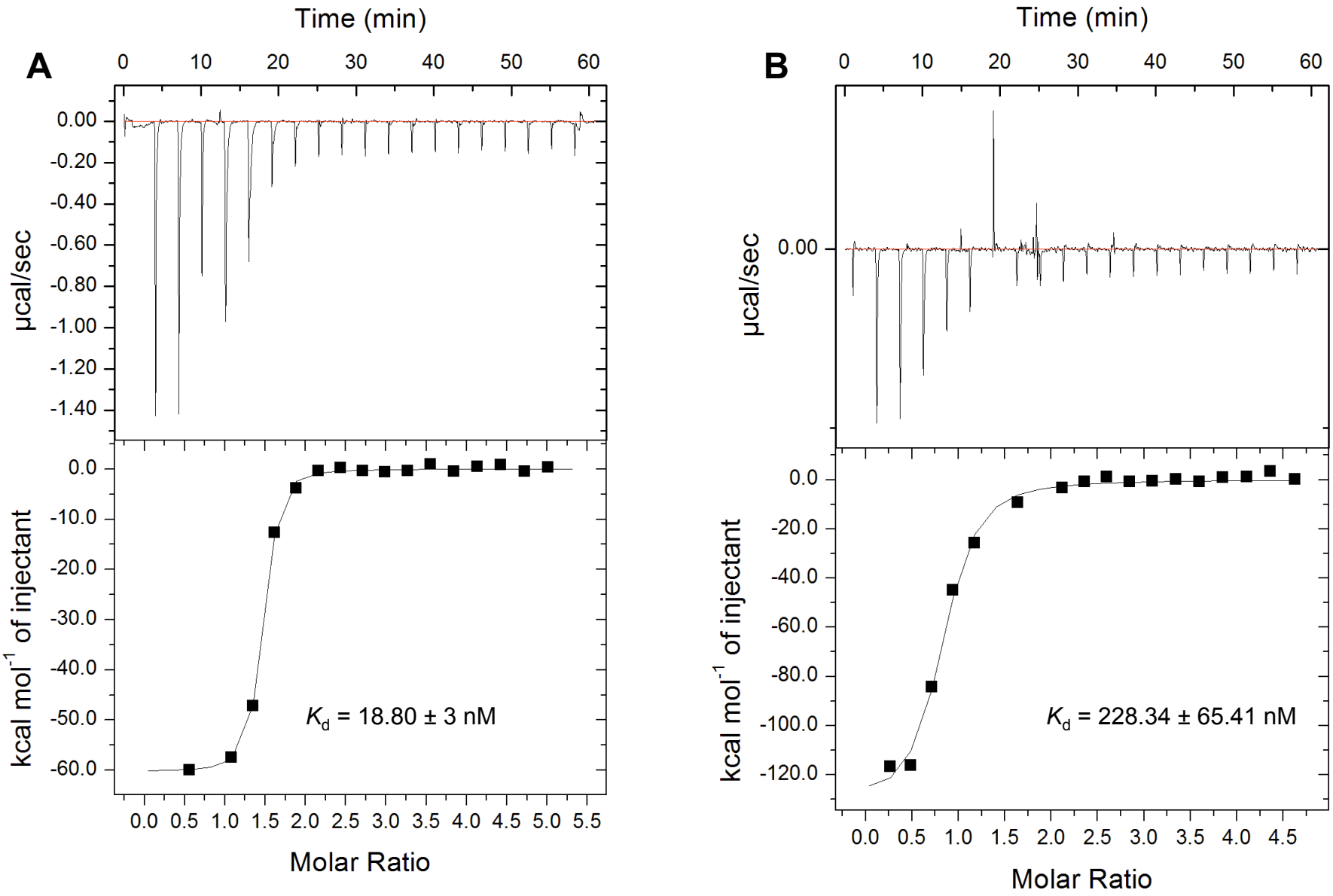

Supplementary Figure S2. miR-122 interactions with Site 1 and Site 2 of the HCV RNA. Isothermal titration calorimetry (ITC) thermograms and resulting binding curve of the titration of **(A)** Site 1 (nts 1-27) and **(B)** Site 2 (nts 29-42) of the HCV RNA with miR-122. All data are representative of at least three independent replicates and K_d values are an average of three measurements (±) error propagated from individual fits.

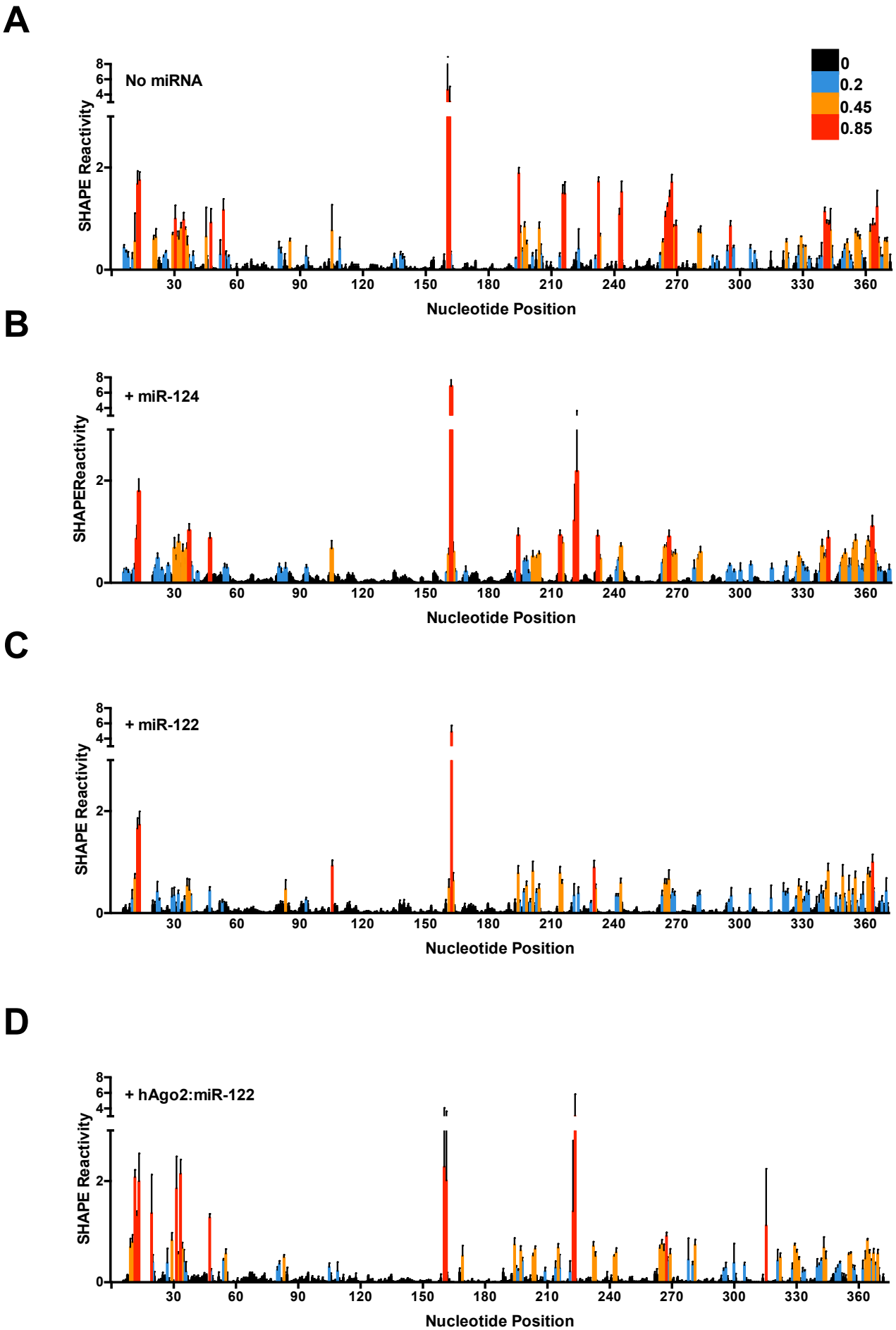
A
No miRNA
SHAPE Reactivity
0
0.2
0.45
0.85
Nucleotide Position
B
+ miR-124
SHAPEReactivity
Nucleotide Position
C
+ miR-122
SHAPE Reactivity
Nucleotide Position
D
+ hAgo2:miR-122
SHAPE Reactivity
Nucleotide Position

Supplementary Figure S3. *In vitro* SHAPE analysis of HCV 5' UTR by capillary electrophoresis. Normalized SHAPE reactivities of nts 1-371 of the HCV RNA with **(A)** no miRNA, **(B)** miR-124, **(C)** miR-122, and **(D)** hAgo2:miR-122. Nucleotides 1-5 and 14-19 were omitted due to high background reactivity. Nucleotides with high (≥ 0.85, red), intermediate (between 0.4 and 0.85, orange), low (between 0.2 and 0.4, blue) and very low (≤ 0.2, black) SHAPE reactivity are indicated. The data represents the results of at least four independent replicates and error bars represent the standard error of the mean (SEM).

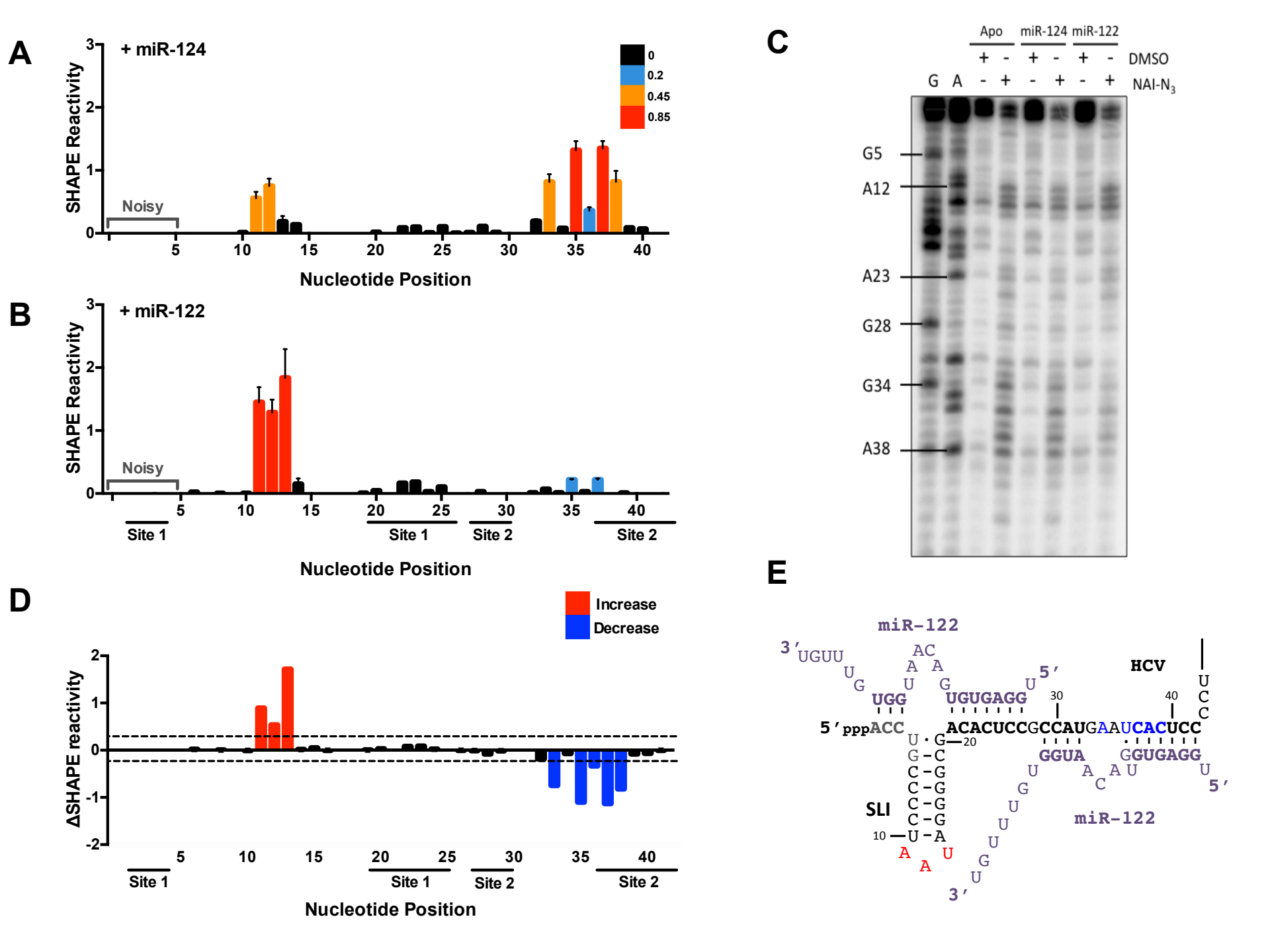
A
+ miR-124
SHAPE Reactivity
0
0.2
0.45
0.85
Noisy
Nucleotide Position
B
+ miR-122
SHAPE Reactivity
Noisy
Site 1
Site 1
Site 2
Site 2
Nucleotide Position
C
Apo
miR-124
miR-122
DMSO
NAI-N3
G A
G5
A12
A23
G28
G34
A38
D
Increase
Decrease
ΔSHAPE reactivity
Site 1
Site 1
Site 2
Site 2
Nucleotide Position
E
miR-122
3′UGUU
AC
A A
U G
U G
U
5′
HCV
UGG
UGUGAGG
30
40
U
C
C
5′pppACC
ACACUCCGCCAUGAAUCACUCC
U·G
20
G-C
GGUA
GGUGAGG
C-G
U
A
A U
U
C-G
G
C
5′
SLI
C-G
U
C-G
U
miR-122
10
U-A
U
A
A
U
G
U
3′

Supplementary Figure S4. *In vitro* SHAPE analysis of HCV RNA by gel electrophoresis. (A) Normalized SHAPE reactivity of 1-42 nt HCV RNA with miR-122 and **(B)** miR-124 (control). Nucleotides 1-5 were omitted due to high background reactivity. Nucleotides with high (≥ 0.85, red), intermediate (between 0.4 and 0.85, orange), low (between 0.2 and 0.4, blue) and very low (≤ 0.2, black) SHAPE reactivity are indicated. **(C)** Representative SHAPE analysis by gel electrophoresis of HCV RNA with miR-122 and miR-124 (control) **(D)** Graph showing the changes in SHAPE reactivity upon miR-122 binding, ΔSHAPE = miR-122 reactivity – miR-124 reactivity. Significant increases (above baseline, red) and decreases in reactivity (below baseline, blue) are indicated. **(E)** Changes in reactivity upon miR-122 binding are shown on the miR-122: HCV RNA secondary structure model, coloured as in **(D)**. Data is representative of at three independent replicates and error bars represent the standard error of the mean (SEM).

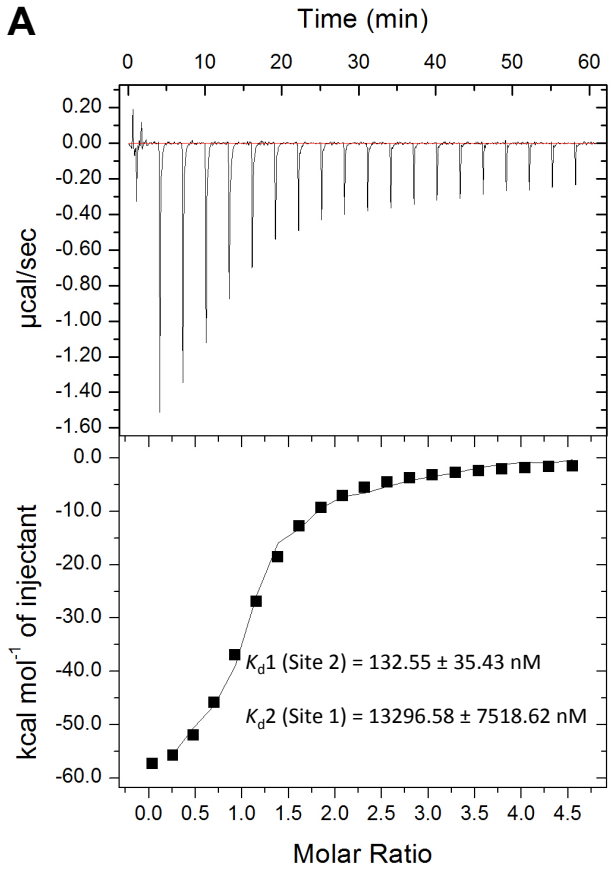
A
Time (min)
µcal/sec
kcal mol-1 of injectant
Kd1 (Site 2) = 132.55 ± 35.43 nM
Kd2 (Site 1) = 13296.58 ± 7518.62 nM
Molar Ratio

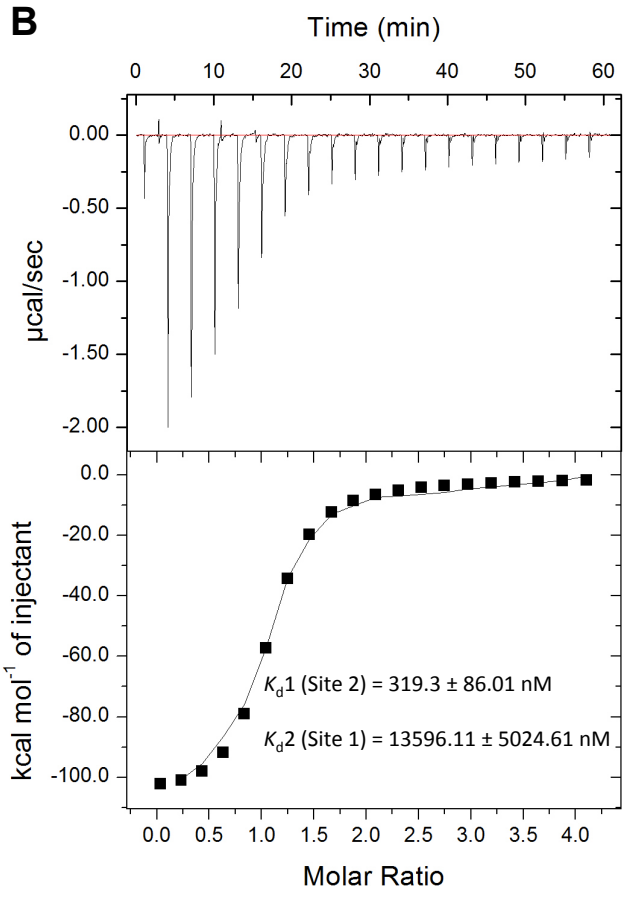
B
Time (min)
µcal/sec
kcal mol-1 of injectant
Kd1 (Site 2) = 319.3 ± 86.01 nM
Kd2 (Site 1) = 13596.11 ± 5024.61 nM
Molar Ratio

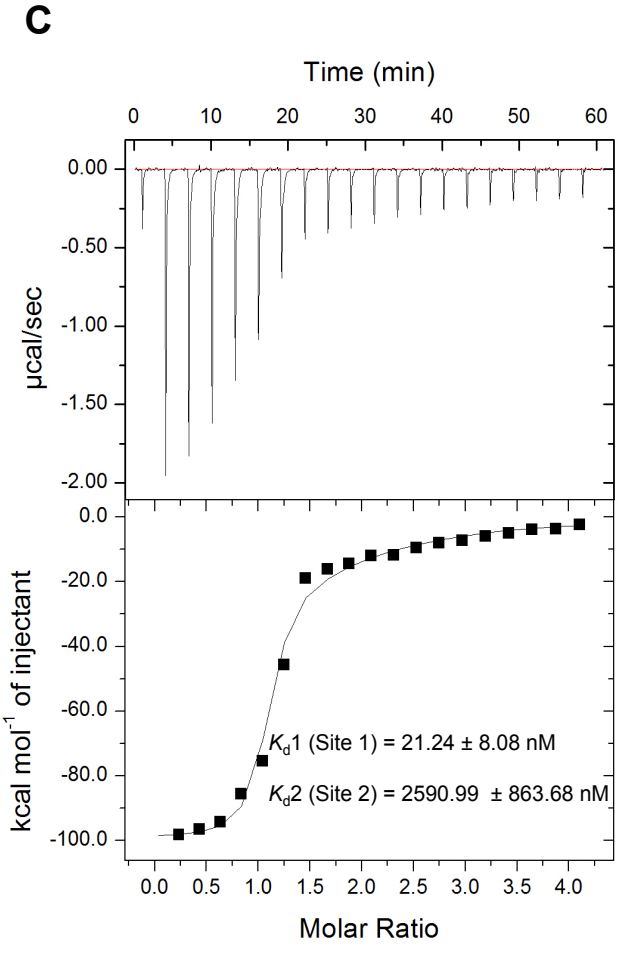
C
Time (min)
µcal/sec
kcal mol-1 of injectant
Kd1 (Site 1) = 21.24 ± 8.08 nM
Kd2 (Site 2) = 2590.99 ± 863.68 nM
Molar Ratio

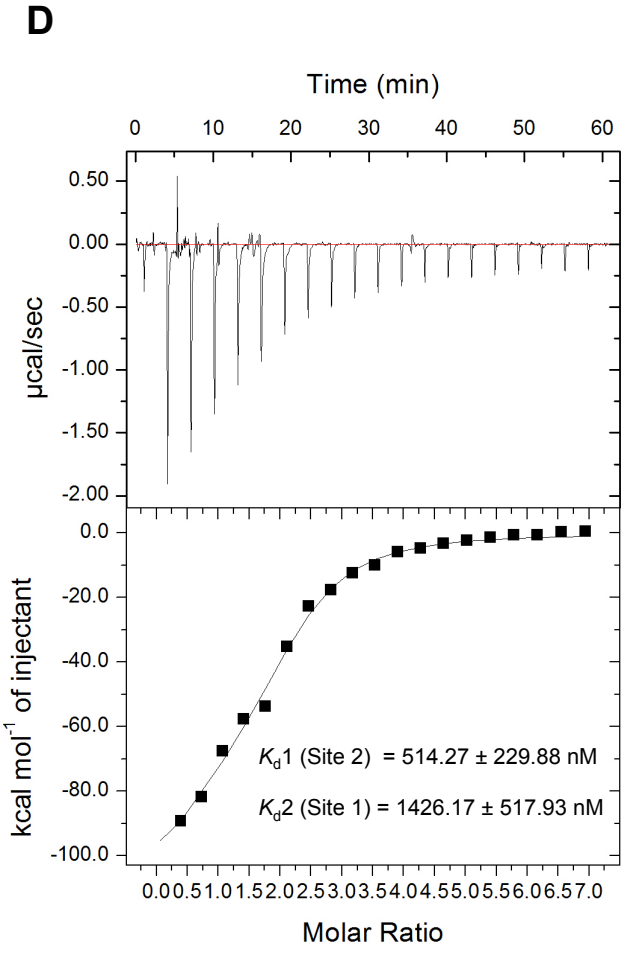
D
Time (min)
µcal/sec
kcal mol-1 of injectant
Kd1 (Site 2) = 514.27 ± 229.88 nM
Kd2 (Site 1) = 1426.17 ± 517.93 nM
Molar Ratio

Supplementary Figure S5. miR-122 interactions with WT, S2p5,6, G28A 1-117 nt and WT 1-371 nt HCV RNA. Isothermal titration calorimetry (ITC) thermograms and resulting binding curve of the titration of miR-122 with 1-117 nt **(A)** WT, **(B)** Site 2 p5,6, and **(C)** G28A HCV RNA as well as with **(D)** 1-371 WT HCV RNA. All data are representative of at least three independent replicates and K_d values are an average of three measurements (±) error propagated from individual fits.

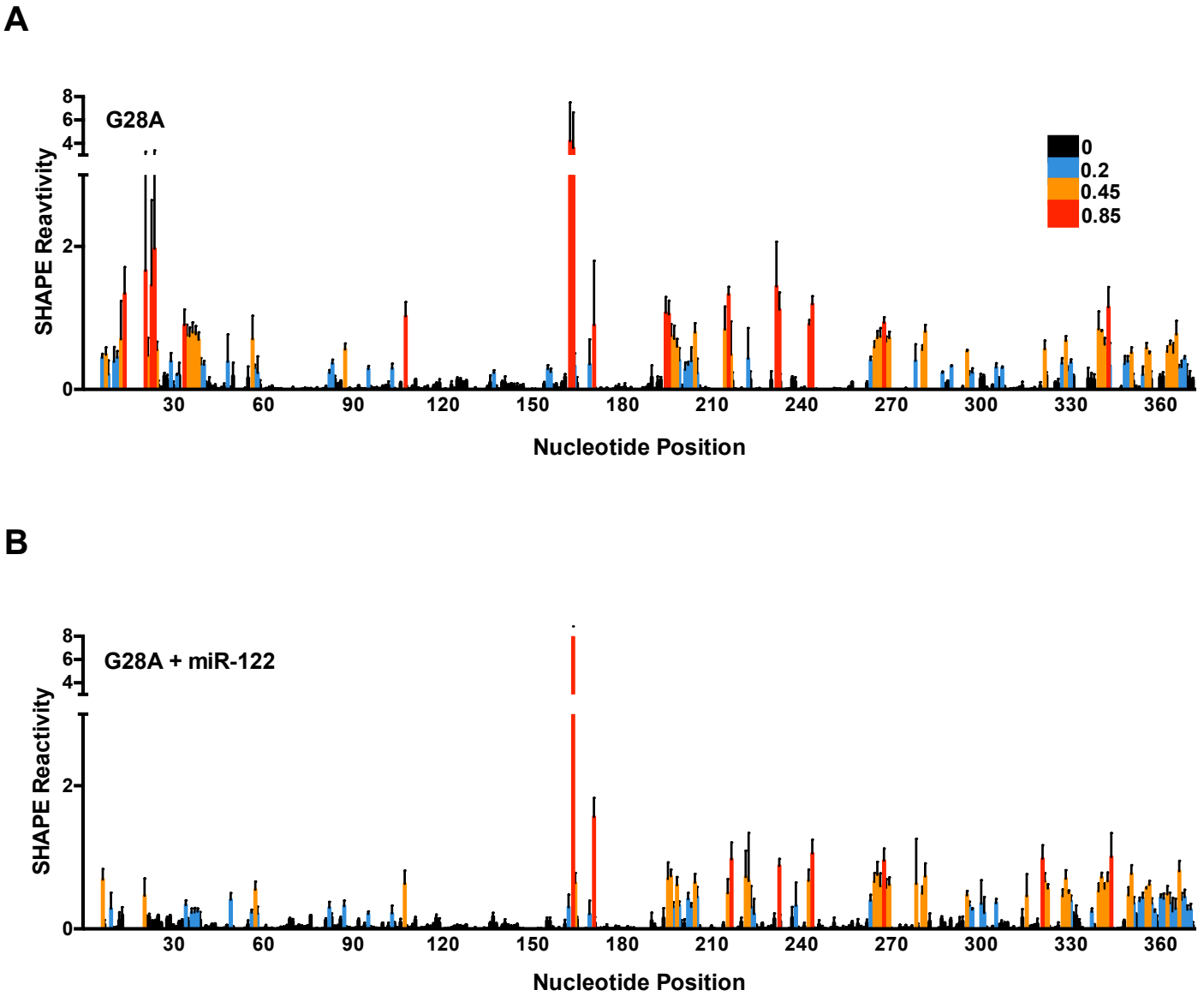

Supplementary Figure S6. *In vitro* SHAPE analysis of G28A 5' UTR by capillary electrophoresis. Normalized SHAPE reactivities of nts 1-371 of the G28A HCV RNA with **(A)** no miRNA or **(B)** + miR-122. Nucleotides 1-5 and 14-19 were omitted due to high background reactivity. Nucleotides with high (≥ 0.85, red), intermediate (between 0.4 and 0.85, orange), low (between 0.2 and 0.4, blue) and very low (≤ 0.2, black) SHAPE reactivity are indicated. The data represents the results of four independent replicates and error bars represent the standard error of the mean (SEM).

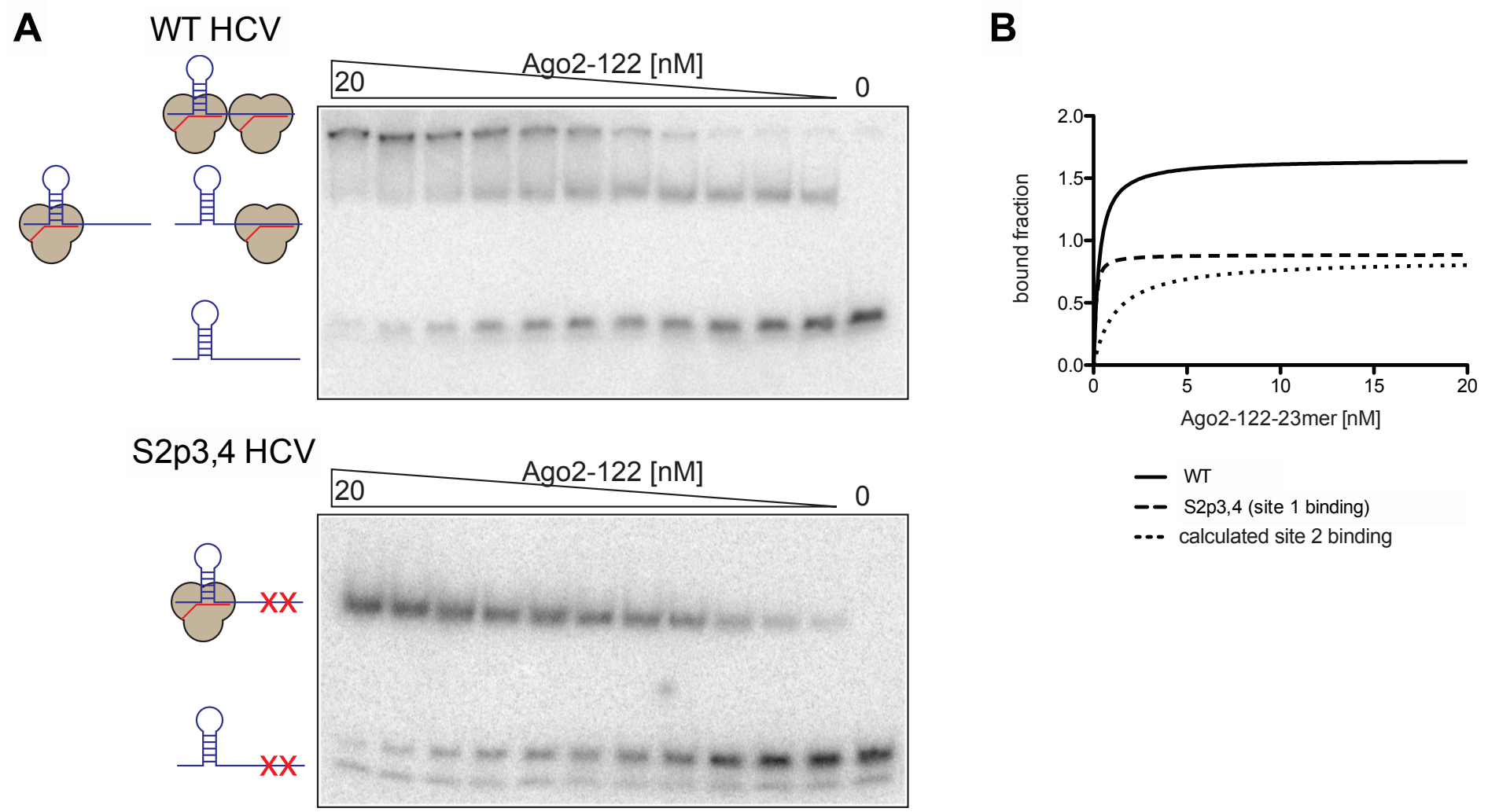

Supplementary Figure S7. Determination of dissociation constants for the Ago2:miR-122 HCV complexes. (A) Examples of electrophoretic mobility shift assay results used for the binding data in **Figure 4B**. Recombinantly expressed hAgo2 loaded with miR-122 (final concentration: 20, 10, 5, 2.5, 1.25, 0.625, 0.3125, 0.15625, 0.078125, 0.0390625, 0.01953125, and 0 nM) was incubated with radiolabeled viral RNA comprising nts 1-42 of WT (top) or S2p3,4 HCV RNA. Single and double shifts are indicated by cartoons. The depicted gels are one of three independent replicates.
(B) Equilibrium binding curves for Ago2:miR-122 and WT (two binding sites), S2p3,4 (Site 1), and the calculated Site 2 (WT minus Site 1) HCV RNA, using Equation 1 (*see* Materials & Methods).

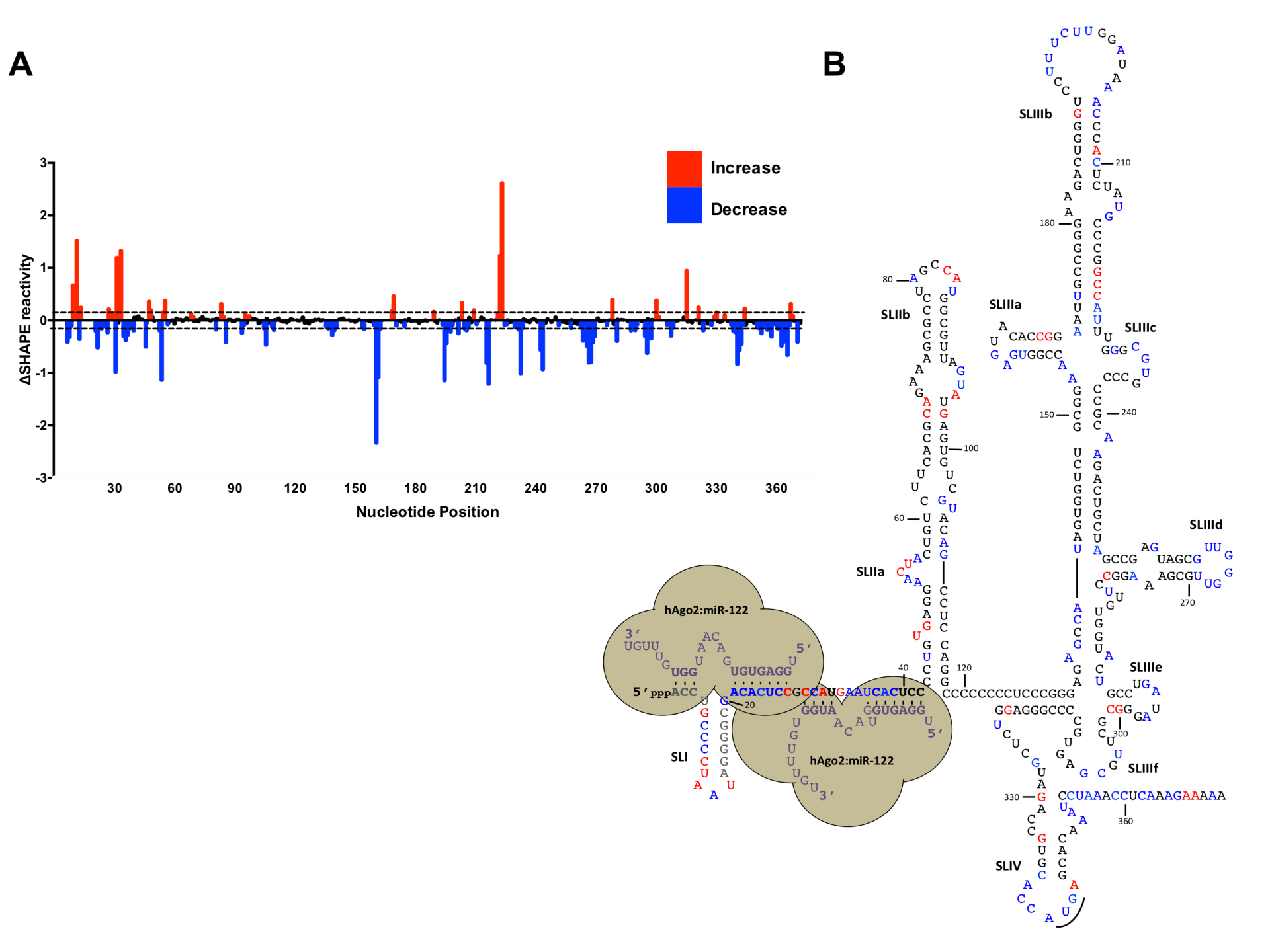
A
B
Increase
Decrease
ΔSHAPE reactivity
Nucleotide Position
hAgo2:miR-122
SLI
SLIIa
SLIIb
SLIIIa
SLIIIb
SLIIIc
SLIIId
SLIIIe
SLIIIf
SLIV

Supplementary Figure S8. Changes in SHAPE reactivity upon hAgo2:miR-122 binding to the entire HCV 5' UTR. (A) Difference plot showing changes in SHAPE reactivity upon hAgo2:miR-122 binding, ΔSHAPE = hAgo2:miR-122 reactivity – HCV RNA reactivity. Significant increases (above baseline, red) and decreases in reactivity (below baseline, blue) are indicated. **(B)** Changes in reactivity upon hAgo2:miR-122 binding are superimposed onto the secondary structure of the HCV 5' UTR (coloured as in **(A)**).